Permafrost hydrology in changing climatic conditions: seasonal variability of stable isotope composition in rivers in discontinuous permafrost

Environmental Research Letters

LETTER

CrossMark

Permafrost hydrology in changing climatic conditions: seasonal variability of stable isotope composition in rivers in discontinuous permafrost

Dmitry A Streletskiy[1], **Nikita I Tananaev**[2], **Thomas Opel**[3], **Nikolay I Shiklomanov**[1], **Kelsey E Nyland**[1], **Irina D Streletskaya**[4], **Igor' Tokarev**[5] **and Alexandr I Shiklomanov**[6]

[1] Department of Geography, The George Washington University, 1922 F St. NW, Washington, DC, 20052, USA
[2] Permafrost Institute, Siberian Branch, Russian Academy of Science, Bldg. 8A, 1st District, Igarka, Krasnoyarsk Krai 663200, Russia
[3] Alfred Wegener Institute Helmholtz Centre for Polar and Marine Research, Periglacial Research section, Telegrafenberg A43, D-14473 Potsdam, Germany
[4] Faculty of Geography, Lomonosov Moscow State University, Leninskie Gory, GSP-1, Moscow, 119991, Russia
[5] Research Center 'Geomodel', Saint-Petersburg State University, Peterhoff, Ul'yanovskaya ul., 1, Saint-Petersburg, 198504, Russia
[6] Earth Systems Research Center, University of New Hampshire, Morse Hall, 8 College Rd, Rm. 211, Durham NH 03824, USA

E-mail: strelets@gwu.edu

Abstract

Role of changing climatic conditions on permafrost degradation and hydrology was investigated in the transition zone between the tundra and forest ecotones at the boundary of continuous and discontinuous permafrost of the lower Yenisei River. Three watersheds of various sizes were chosen to represent the characteristics of the regional landscape conditions. Samples of river flow, precipitation, snow cover, and permafrost ground ice were collected over the watersheds to determine isotopic composition of potential sources of water in a river flow over a two year period. Increases in air temperature over the last forty years have resulted in permafrost degradation and a decrease in the seasonal frost which is evident from soil temperature measurements, permafrost and active-layer monitoring, and analysis of satellite imagery. The lowering of the permafrost table has led to an increased storage capacity of permafrost affected soils and a higher contribution of ground water to river discharge during winter months. A progressive decrease in the thickness of the layer of seasonal freezing allows more water storage and pathways for water during the winter low period making winter discharge dependent on the timing and amount of late summer precipitation. There is a substantial seasonal variability of stable isotopic composition of river flow. Spring flooding corresponds to the isotopic composition of snow cover prior to the snowmelt. Isotopic composition of river flow during the summer period follows the variability of precipitation in smaller creeks, while the water flow of larger watersheds is influenced by the secondary evaporation of water temporarily stored in thermokarst lakes and bogs. Late summer precipitation determines the isotopic composition of texture ice within the active layer in tundra landscapes and the seasonal freezing layer in forested landscapes as well as the composition of the water flow during winter months.

Introduction

Numerous studies indicate that Northern Eurasia is experiencing increases in air temperature (Fedorov *et al* 2014), reductions in sea ice cover (Stroeve *et al* 2012), a lengthened ice-free period in lakes and rivers (AMAP 2011, Shiklomanov and Lammers 2014), and landcover and ecosystem changes (Bhatt *et al* 2010, Callaghan *et al* 2011). Observations of river discharge from the six largest Russian rivers, all flowing into the Arctic Ocean (Northern Dvina, Pechora, Ob, Yenisei, Lena, and Kolyma), have shown a 7% increase in discharge over the 1936–1999 period (Peterson *et al* 2002). Recent studies showed an increase in the annual discharge of these six large Eurasian rivers to be 2.7 km^3 yr^{-1} or 210 km^3 over the

period 1936–2010, with winter discharge contributing about 70% of this increase, i.e. $1.9 \, km^3 \, yr^{-1}$ or $146 \, km^3$ (Shiklomanov and Lammers 2013). One peculiarity of Eurasian Arctic rivers is the presence of permafrost which underlies extensive areas of these watersheds. Over the last three decades, permafrost in the Eurasian Arctic has begun to experience warmer ground temperatures (Romanovsky *et al* 2010), and thickening of the active layer (Shiklomanov *et al* 2012) leading to decreased permafrost extent (Oberman and Shesler 2009, Streletskiy *et al* 2014). Permafrost degradation has been associated as a potential cause of the observed increases in winter baseflow in some Arctic rivers (McClelland *et al* 2004), but permafrost degradation could also lead to increased groundwater storage and hence a reduction in river discharge.

One of the challenges to evaluating the effects of permafrost degradation, and the potential northward migration of discontinuous permafrost, on river flow is the large number of possible responses of the hydrological systems to changing permafrost conditions. For example, a recent study found that melting ground ice in discontinuous permafrost was not a source of observed changes in river discharge, but rather the thickening of the active layer was more significant to the changing watershed hydrology (Landerer *et al* 2010). Geochemical and isotope compositions of precipitation, groundwater, rivers, lakes and ground ice may help to distinguish between various sources of water in hydrological systems, assuming that the different sources have distinct stable water isotope compositions (Klaus and McDonnell 2013, Lacelle and Vasil'chuk 2013). Various mixing scenarios between different sources define the isotopic compositions of water in a river. For example, it was shown that the seasonal stable isotope composition of two small rivers in Northeastern Russia follow the isotopic composition of precipitation very closely (Huitu *et al* 2013). Several studies have revealed significant changes in the isotopic composition of river water during the spring snowmelt period, as snow cover has a lower isotopic composition relative to rain (Welp *et al* 2005, Sugimoto and Maximov 2012, Huitu *et al* 2013). Studies conducted in the Kolyma and Mackenzie river watersheds (Welp *et al* 2005, Yi *et al* 2010) were able to trace the effects of surface water evaporation in wetlands, bogs, and thermokarst lakes prior to entering the river flow in summer, while a study of the Lena river did not show that river flow was affected by evaporation of surface water (Sugimoto and Maximov 2012).
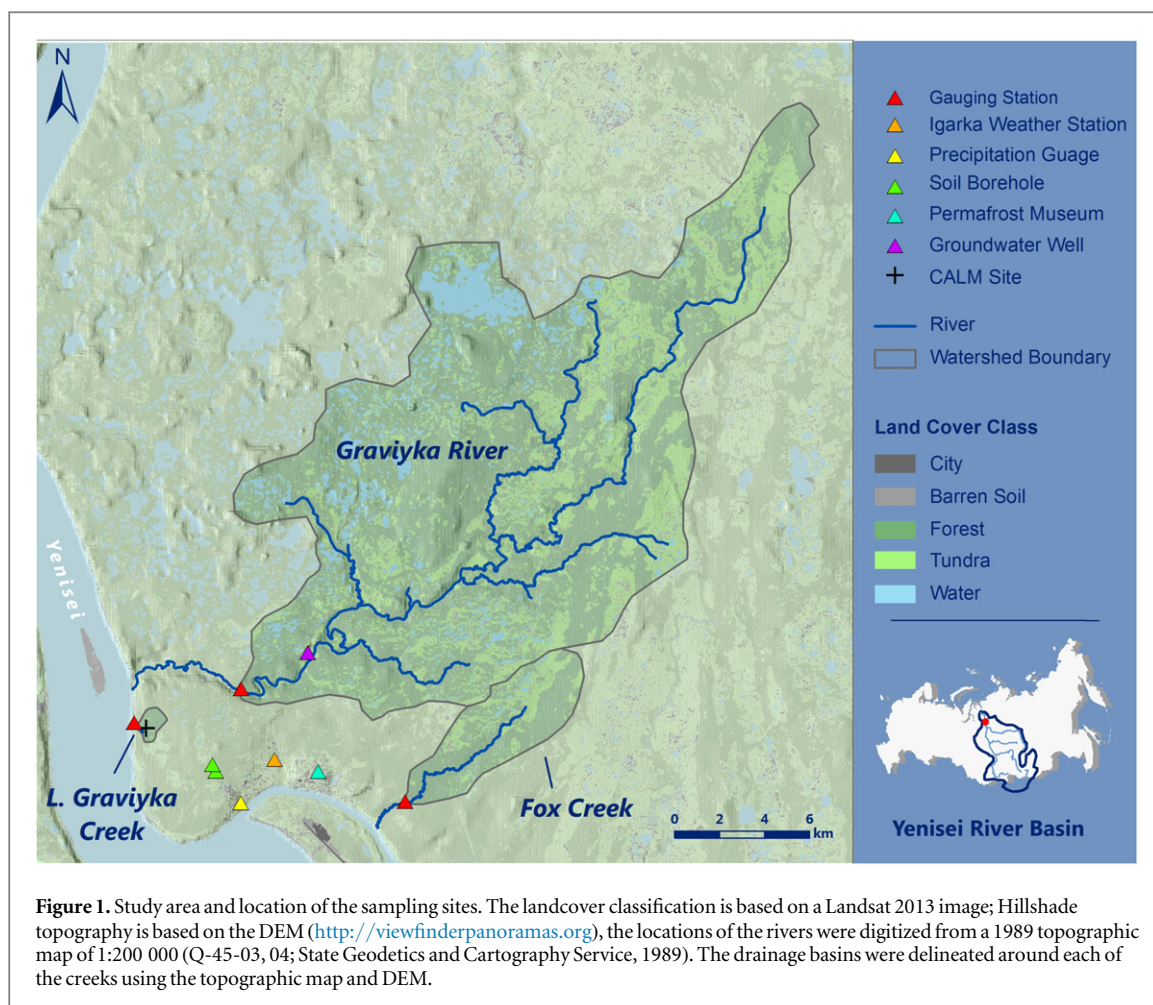
Although studies have investigated the effects of changing permafrost conditions on the hydrological regime at local (Quinton and Baltzer 2013), regional (Walvoord and Striegl 2007, St Jacques and Sauchyn 2009, Sjöberg *et al* 2013) and circumpolar scales (Yi *et al* 2012), studies of the stable isotopic composition of rivers from the Eurasian Arctic are rare, even though this region contains three of the four major Arctic rivers (Shiklomanov *et al* 2013) and contributes 74% of the total terrestrial runoff to the Arctic Ocean (McClelland *et al* 2006). This study aims to: (i) determine the possible effects of changing climatic conditions on river discharge from 1970 to 2014 for watersheds situated near the town of Igarka in the lower Yenisei River region; and (ii) identify the sources of water contributing to 2013–14 river flow on seasonal scale. The study area is located at the transition between continuous and discontinuous permafrost on relatively shallow, ice-rich permafrost with temperatures close to the melting point. This makes the permafrost in this area sensitive to changes in climatic and environmental conditions, and offers the potential to evaluate the effects of changing permafrost conditions on hydrological regime of rivers and creeks draining to the Yenisei River.

Study area

The study area is located in the vicinity of the town of Igarka, 120 km North of the Arctic Circle, on the right bank of the Yenisei River (figure 1). The climate of the region can be classified as Continental subarctic climate (*Dfc*) (Peel *et al* 2007) with low winter temperatures and a relatively warm summer. The mean annual air temperature is $-7.6 \, °C$ for the 1973–2013 period. The coldest month is January ($-27.6 \, °C$) and the warmest month is July ($+15.0 \, °C$). The region receives 513 mm of precipitation annually, with 70 days of rain and 130 days of snow per year. Seasonal snow cover is established by early October and melts by mid-June. The regional average snow depth is 0.7–1.0 m, but can exceed 1.5 m in topographic depressions.

The region is located at the boundary between continuous and discontinuous permafrost and is characterized by Pleistocene and Holocene age permafrost reflective of the complex history of sedimentation and landscape development (Rodionov *et al* 2007, Flessa *et al* 2008). On the third Yenisei terrace at 50–60 m asl underlain by predominantly limnic fine-textured sediments, permafrost formed during the Zyryan epoch (Early Weichselian, 71 000–57 000 years BP, MIS 4 (Bassinot *et al* 1994)). During Kargino interstadial (57 000–24 000 years BP, MIS 3) widespread permafrost degradation occurred. Subsequent cooling during the Sartan stadial (Late Weichselian, MIS2, Last Glacial Maximum) resulted in syngenetic freezing of the coarse alluvial and fluvioglacial sediments of the second Yenisei terrace at 30–40 m asl (Astakhov and Mangerud 2007). The degradation of continuous Pleistocene permafrost during the Holocene Climatic Optimum was accompanied by the formation of numerous peat bogs and subsequent permafrost aggradation in organic-rich soils during the colder Holocene periods (Astakhov and Isaeva 1988). As a result two distinct permafrost layers are present in the area: deeper Pleistocene permafrost with its table at 3–5 m depth, and near-surface Holocene permafrost

Figure 1. Study area and location of the sampling sites. The landcover classification is based on a Landsat 2013 image; Hillshade topography is based on the DEM (http://viewfinderpanoramas.org), the locations of the rivers were digitized from a 1989 topographic map of 1:200 000 (Q-45-03, 04; State Geodetics and Cartography Service, 1989). The drainage basins were delineated around each of the creeks using the topographic map and DEM.

with its table at 0.4–1.5 m depth, depending on soil and vegetation conditions. The age-related depth to permafrost is relatively well identified by differences in landscape conditions (Tyrtikov 1964 Rodionov *et al* 2007). The near-surface Holocene permafrost layer is present under moss-, grass- and sedge-dominated tundra landscapes formed on organic-rich fine lacustrine (limnic) sediments. Relatively dense taiga forests, formed on better-drained sandy and loamy soils, are dominated by larch (*Larix Siberica*), birch (*Betula Pendula*), and Siberian pine (*Pinus Siberica*). These landscapes, with the exception of steep North-facing slopes, are underlain only by the deeper Pleistocene permafrost (Rodionov *et al* 2007).

The total permafrost thickness varies between 10 and 40 m depending on the presence of the near-surface Holocene permafrost layer (Kuznetsova *et al* 1985). Throughout the area permafrost temperature is around −1.0 to −0.1 °C. The gravimetric ground ice content ranges from 35 to 40% in mineral soils to 60% and higher in peatlands, floodplains, and drained thermokarst lake basins (a.k.a alas depressions). Observations, conducted in a deep permafrost tunnel under the Igarka Permafrost Museum (http://igarka-permafrostmuseum.ru/) show that between 3 and 20 m depth there is an extensive network of ice

lenses formed in glacio-lacustrine sediments and reaching 0.3 m in thickness and 8 m in length (Shur and Zhestkova 2003).

Poor drainage and relatively high ground ice content of limnic tundra sediments promotes the development of thermokarst lakes that dot the landscape. The groundwater table is located at various depths depending on the local topography. The reported values range from 6 to 17 m in the floodplains to 15–30 m on fluvial terraces (Vasil'chuk 1989). Several small rivers and streams dissect the study area and drain into the Yenisei River. The major contribution to streamflow comes from snowmelt followed by summer precipitation. Groundwater base flow is present in larger streams.

Data and methods

Field investigations were conducted over the 2013–2014 period at three watersheds within the 500 km^2 study area. The three watersheds include: Graviyka, Fox Creek, and Little Graviyka that drain into the Yenisei River. Watersheds of different sizes were selected to represent a range of stream sizes and environmental conditions found within the region (figure 1):

Graviyka is the largest stream out of the three studied with a watershed occupying more than 320 km^2 primarily within the second and third Yenisei River terraces. Two thirds of the watershed is covered by forest while a quarter of the basin is characterized by tundra landscapes, affected by shallow Holocene permafrost. Numerous small lakes and bogs occupy the upper portion of the Graviyka basin. A small portion of the watershed is covered by non-vegetated surfaces, predominantly sand blowouts.

Fox Creek is a medium size stream located mostly within the second Yenisei terrace with a 25 km^2 watershed. While the relative proportion of forested and permafrost-affected tundra landscapes are similar to Graviyka, a significantly smaller portion of the Fox Creek basin is occupied by lakes as the second Yenisei terrace is primarily composed of alluvial and glacio-fluvial sediments formed during Kargino interstadial (MIS 3) and is well drained.

Little Graviyka is the smallest stream with a watershed of about 1 km^2. It is located on the narrow permafrost dominated first terrace of the Yenisei River at 20–40 m asl formed primarily during Sartan stage (MIS2).

Climatic and permafrost characteristics

Daily meteorological data (air temperature, precipitation, and snow height, and soil temperature) were obtained from NCDC GSOD for the Igarka weather station (WMO ID 23274, 67.47 N, 86.57 E, 20 m a.s.l.). Daily soil temperature data were available at standard depths of 0.2, 0.4, 0.8, 1.6, and 3.2 m for 1977–2014.

Active layer thickness data are available for 2008–2014 from the Circumpolar Active Layer Monitoring (CALM) R40 site (Zepalov *et al* 2008, Sergievskaya *et al* 2012) located 5 km North–West from Igarka (http://gwu.edu/~calm). The site is representative of two main landcover classes found in the area.

Permafrost temperature at 0.5, 3.0, 5.0 and 10 m depths were monitored at two GTN-P boreholes: Graviyka1 and Graviyka2, representing forest and tundra landscapes respectively, in the vicinity of the CALM site (http://gtnpdatabase.org/). Temperatures in both boreholes were recorded every 4 h at 0.5, 3.0, 5.0 and 10 m depths using Onset U12 4-channel temperature loggers.

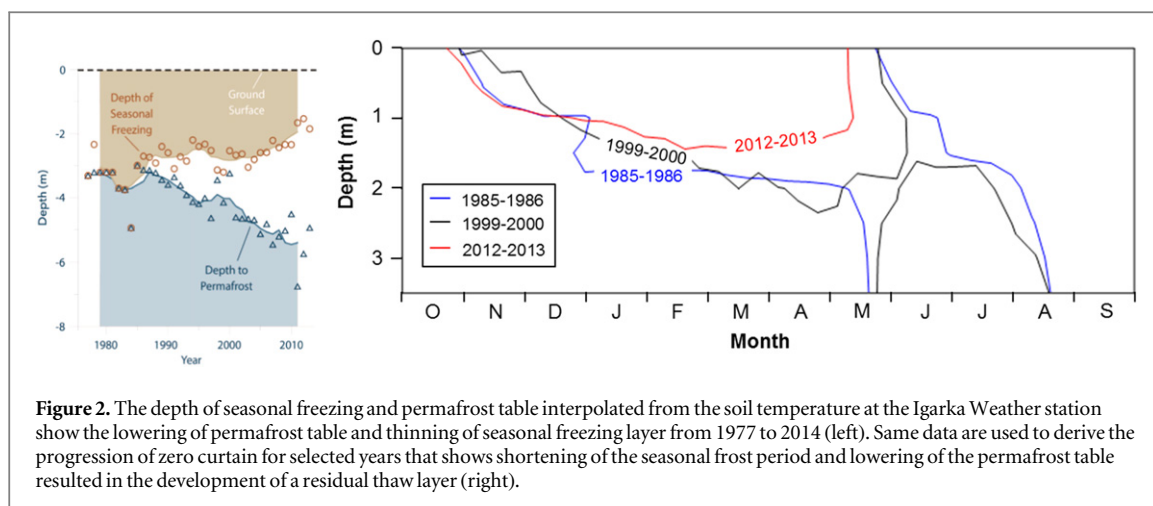### Landcover classification and temporal change

In order to perform the landcover classification for the three studied drainage basins, the location of the creeks were first digitized from a 1989 topographic map (Q-45-03, 04; State Geodetics and Cartography Service, 1989) (1:200,000 scale) and verified using Google Earth imagery from 2012. The drainage basins were then delineated around each of the creeks using the topographic map and an ASTER GDEM V2 digital elevation model.

Landsat TM-based 30 m resolution imagery was used to create landcover classification maps for the study area to assess 30 year changes in areal extent of shallow permafrost-affected landscapes for each watershed of this study. A modified version of the methodology known as 'Landsat dense time stacking,' was used to classify Landsat imagery for the area containing the three basins previously delineated (Schneider 2012, Nyland 2015). The method works by stacking all available scenes, including those normally rejected due to date or obscuring cloud cover, with the thought that enough scenes will compensate for data gaps. For this work, all available Landsat 5 and 8 scenes were downloaded from the USGS Global Visualization Viewer (http://glovis.usgs.gov/) and georectified as needed. Using ERDAS Imagine 2013 and ArcGIS 10.1 software, NDVI was applied to each scene in the 1985–1987 and 2013–2014 time periods. All NDVI images were stacked and the maximum value for each pixel extracted. The resulting images of maximum NDVI per pixel represent a composite of the least cloud affected pixels. Using 15 training sites per class, the maximum and minimum NDVI values were used in a conditional statement to classify the entire scene into a thematic map. Lastly, an accuracy assessment was performed for the later period using high resolution imagery and ground truth data collected using GPS units within the study area during the summer of 2013. A 2006 Quickbird scene was used for this 2013–14 classification accuracy assessment. While not from the time period this was the best high resolution scene that could be obtained in proximity to the time period of interest. The assessment yielded an overall accuracy of 83.33%.

Hydrological characteristics

Water flow was measured four times at Fox Creek and Little Graviyka gauging stations during the summer using flow probe ISP 1 M (Russia) and Flow Probe FP201—Global Water (USA) at 0.2, 0.6, and 0.8 m depths with 5% accuracy. Daily discharges were calculated based on rating curves established for each gauging station. Water levels were measured with portable loggers by Global Water (USA) at Graviyka River and Fox Creek gauging station during the summers of 2013 and 2014, however malfunctioning loggers prevented the use of these data and were therefore excluded from the paper. Therefore discharge data from the Hydrograph Hydrological Model specifically parameterized for the Graviyka watershed were used in the absence of observed discharge data during the sampling period (Lebedeva *et al* 2014).

Historical daily discharges available for Graviyka River gauging stations were digitized from the Hydrological Yearbooks from 1940 to 1994 and have the most complete records during the 1973–1990 period when only few days had missing observations. Electrical conductivity (EC) and pH were measured using

Figure 2. The depth of seasonal freezing and permafrost table interpolated from the soil temperature at the Igarka Weather station show the lowering of permafrost table and thinning of seasonal freezing layer from 1977 to 2014 (left). Same data are used to derive the progression of zero curtain for selected years that shows shortening of the seasonal frost period and lowering of the permafrost table resulted in the development of a residual thaw layer (right).

Global Water EC500 *in situ* only at Graviyka River at the same time that water samples were collected for isotope analysis. The accuracy is 2 μS for EC and $\pm$0.01 for pH.

Water samples for stable isotope analysis

Water samples for the stable isotope analysis were collected from various water sources within the study area during 1 January 2013 to 1 October 2014 period. Samples of stream water were collected at 1 to 10 day intervals, depending on the rate of change in hydrologic conditions and sites' accessibility. Samples of precipitation (rain and snow) were collected to establish the local meteoric water line (LMWL). Additional snow samples were collected from all three watersheds near the corresponding gauging stations during the winter 2013/14. To determine the stable isotope composition of the upper permafrost and seasonally frozen layer, six 1.2 m long cores were extracted from boreholes drilled. Three cores represented near-surface permafrost in tundra landscape and three represented the seasonally frozen layer within the birch-larch forest (figure 1). Additional ground ice samples were obtained in the permafrost tunnel under the Igarka Permafrost Museum at depths of 4.5, 7.5 and 10 m. To determine the influence of summer evaporation and potential ground ice contribution to the isotope composition of the water, samples were collected from thermokarst lakes and bogs, and from a ground water spring located in Graviyka watershed. The location of sampling sites is shown in figure 1. A detailed description of sampling procedures is given in appendix.

All collected water samples were analyzed at the Core Facility RC 'Geomodel' at St. Petersburg State University, Russia using cavity ring-down spectroscopy (Picarro L-2120i). Both δ^{18}O and δD were determined for the same water sample. The resulting values were expressed in δ-notation relative to the Vienna Standard Mean Ocean Water (VSMOW2). The precision of the method is $\pm$0.1‰ for δ^{18}O and $\pm$1.0‰ for δD.

Results and discussion

Changes in ground temperature and active layer thickness

An increase in mean annual air temperature of 0.4 °C/decade was observed at the Igarka weather station over the last forty years. The increase is attributed primarily to spring months. Annual precipitation has not experienced significant change over the same period, however, starting in 2000, precipitation increased slightly relative to the long-term mean. The long-term increase in regional air temperature, accompanied by recent increase in snow cover can contribute to the degradation of relatively warm and thin permafrost within the study area. Daily permafrost temperature observations are available from two boreholes within the study area for 2006–2013. Mean annual ground temperature at 10 m depth is −0.25 °C within forested areas and −0.20 °C in tundra landscapes suggesting that permafrost is near the melting point.

Although there are no long-term direct permafrost observations within the study area, several lines of evidence suggest widespread permafrost degradation throughout the area which manifested itself through the decrease of permafrost extent, thermokarst development, thickening of the active-layer, and increases in soil temperature.

The long-term (1977–2014) soil temperatures at several depths (up to 3.2 m) are available from the weather station located in the town of Igarka. Observations are conducted at a standard meteorological leveled plot under undisturbed vegetation and snow cover conditions. Vegetation is primarily composed of mature seeded grass. While this vegetation cover is not representative of the vegetation within the study area, the data can be used to analyze the general trends of climate-induced changes in the ground thermal regime. The data shows an increase in soil temperature at 3.2 m depth from −0.5 °C in 1970 s to +2.5 °C in 2010 s. Depths of annual thawing and freezing, estimated by polynomial interpolation of temperature data from different depths are shown in figure 2. The

Table 1. Landcover change by watershed from 1985–1987 to 2013–2014.

Watershed	Tundra, %	Taiga, %	Soil, %	Water, %
Graviyka River	−6	+6	0	0
Fox Creek	−4	+5	+1	−1
Little Graviyka Creek	−9	+9	+1	−1

lowering of the permafrost table and the decrease in the depth of seasonal freezing have together promoted development of the residual thaw layer above the permafrost in late 1980s.

Although the response of permafrost to climatic forcings (e.g. temperature, precipitation) in natural tundra landscapes are moderated by thick moss and organic layers, the observed trend can indicate an overall soil temperature change in the Igarka region. This notion is indirectly supported by comparing the landscape-specific active-layer observations collected in the study area during 1950s with those collected at the local CALM site over the period 2008–2014. Although the exact locations of historic measurements are not known, the summary data (Tyrtikov 1964) provide detailed landscape characterizations making it possible to compare the data with modern CALM measurements from similar landscapes. The comparison indicates that from the 1950s to the 2010s the average active-layer thickness has increased from 0.38 m to 0.55 m in tundra landscapes dominated by organic soils.

Changes in landcover

Extensive field work conducted within the study area in the 1950s and 1960s suggests that tundra dominated landscapes are indicative of the presence of Holocene permafrost and that sparse forest landscapes are generally corresponding to areas with a significantly deeper permafrost table associated with Pleistocene permafrost (Tyrtikov 1964). As a result, a generalized landcover classification can be used to assess the spatial distribution of shallow permafrost.

The comparison of landcover classification maps for 1985–1987 and 2013–2014 reveals a decline in the areal extent of tundra predominantly due to the expansion of forested areas (table 1). Such landscape changes can, at least partially, be indicative of permafrost degradation in the Igarka area that occurred over the 30 year period. However, these results should be interpreted with caution as they are less than the reported classification error, even though the probability of capturing noise rather than actual change was minimized by the consistent methodologies used for both time periods.

Changes in hydrological characteristics

The historic observational data were used to show the changes in the hydrological regime in changing climatic conditions; while model estimates of the 2013–14 are used further to identify the sources of water flow on a seasonal scale. Graviyka is the only stream within the study area which has historic (1973–1990) discharge observations. Monthly discharge values were analyzed to assess stream flow seasonality for the 1970s and 1980s. Monthly discharge statistics in $m^3 s^{-1}$ for two periods are presented in table 2. Relative contributions of monthly stream discharges to annual totals for 1973–1981 (1723 $m^3 s^{-1}$) and 1982–1990 (1804 $m^3 s^{-1}$) and relative monthly discharge and precipitation change between the two periods are shown in figure 3. The period 1973–1990 is characterized by decreasing precipitation in all months except August. Simultaneously, a pronounced increase in discharge has occurred over cold (October–April) and snow melt (May) periods. June and July were characterized by decrease in discharge. The increase in May and decrease in June suggest a hydrologic regime shift toward the earlier snowmelt attributable to the spring warming observed during this period.
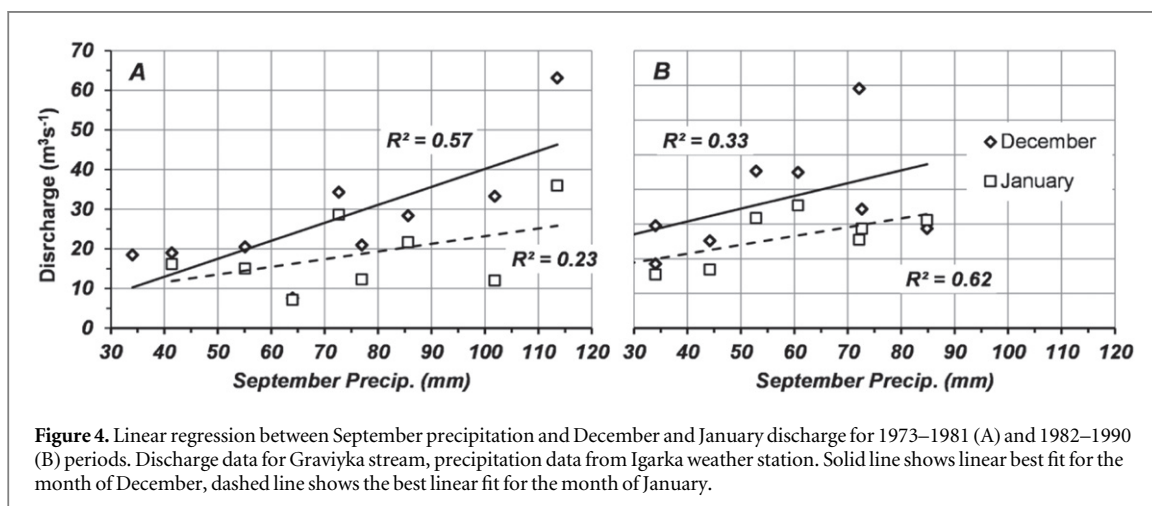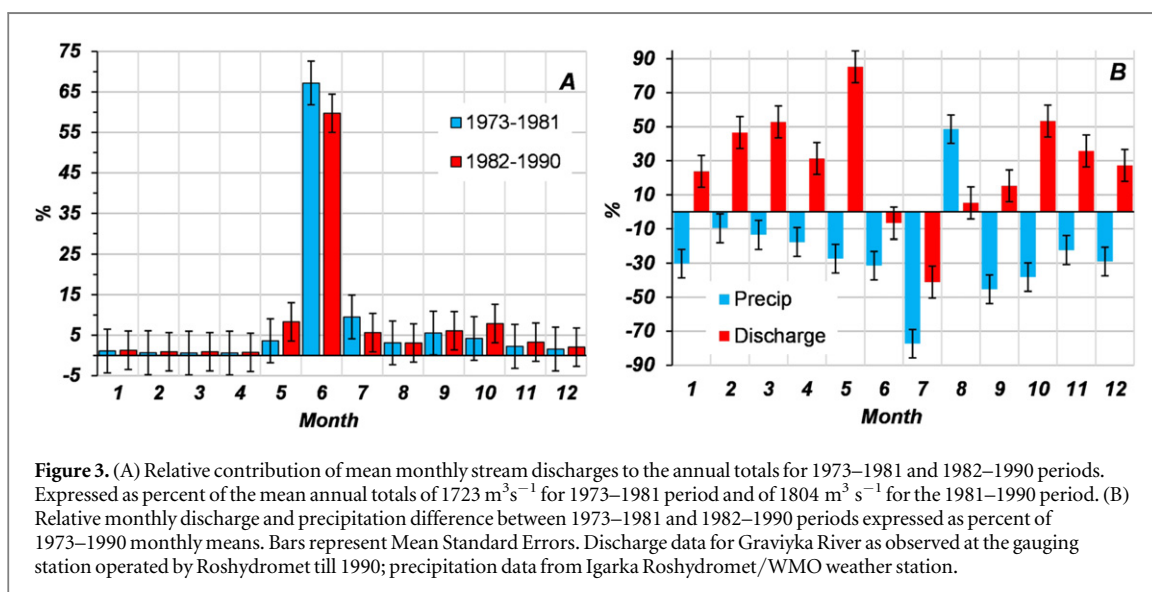
The results of this study indicate that with the exception of spring flooding, rain is the dominant source of water in these streams. To assess the relationship between monthly precipitation and discharge we have used regression analysis for two periods (1970s and 1980s). The results indicate an increase in the time-lag between precipitation events and stream discharge between 1970s and 1980s. During the warm months of the earlier decade there is a positive relationship between precipitation and discharge with a one month time-lag between July precipitation and August streamflow ($R^2 = 0.38$), and August precipitation and September streamflow ($R^2 = 0.61$). For the 1980s, the highest correlation was found for a two-month time-lag between July precipitation and September discharge ($R^2 = 0.71$) and between August precipitation and October discharge ($R^2 = 0.33$). The effect of time-lag produced increases in discharge is most pronounced for September, the last month of consistent liquid precipitation (figure 4). All $R^2 > 0.45$ are statistically significant at $p < 0.10$.

In the 1970s September precipitation was strongly correlated with December discharge ($R^2 = 0.57$), while their influence on January flow was greatly reduced ($R^2 = 0.23$). No correlation was found between September precipitation and February and March flow. For the 1980s, September precipitation contributed to discharge throughout the cold season. The highest correlation was found for January ($R^2 = 0.62$), followed by February ($R^2 = 0.49$), and March ($R^2 = 0.44$).

The estimated annual total discharge during 2013 was 1240 $m^3 s^{-1}$ and 2014 was 2740 $m^3 s^{-1}$. While model estimates cannot be directly compared to the observational data, as the model does not reproduce winter base flow adequately, they give insight to the peculiarities of the hydrological conditions of the two

Table 2. Graviyka stream monthly discharge statistics for 1973–1981 and 1982–1990 nine-year periods. Discharge data as observed at the gauging station operated by Roshydromet till 1990.

MONTH	1	2	3	4	5	6	7	8	9	10	11	12
Discharge statistics (m³ s⁻¹) for the 1973–1981 period												
MEAN	19	11	10	10	65	1145	167	58	96	74	40	27
MAX	36	23	24	26	248	1309	282	167	146	134	97	63
MIN	7	2	4	3	12	842	63	12	17	14	12	8
ST. DEV	9	6	6	7	86	139	76	52	41	38	28	16
Discharge statistics (m³ s⁻¹) for the 1982–1990 period												
MEAN	24	17	17	14	157	1072	110	61	112	127	58	36
MAX	35	28	31	30	315	2006	283	116	223	289	92	69
MIN	14	7	8	6	27	595	40	13	39	18	15	22
ST. DEV	8	8	10	8	112	436	82	39	73	99	26	16

Figure 3. (A) Relative contribution of mean monthly stream discharges to the annual totals for 1973–1981 and 1982–1990 periods. Expressed as percent of the mean annual totals of 1723 m³s⁻¹ for 1973–1981 period and of 1804 m³ s⁻¹ for the 1981–1990 period. (B) Relative monthly discharge and precipitation difference between 1973–1981 and 1982–1990 periods expressed as percent of 1973–1990 monthly means. Bars represent Mean Standard Errors. Discharge data for Graviyka River as observed at the gauging station operated by Roshydromet till 1990; precipitation data from Igarka Roshydromet/WMO weather station.

Figure 4. Linear regression between September precipitation and December and January discharge for 1973–1981 (A) and 1982–1990 (B) periods. Discharge data for Graviyka stream, precipitation data from Igarka weather station. Solid line shows linear best fit for the month of December, dashed line shows the best linear fit for the month of January.

project years. Lower than average discharge in 2013 is attributed to low winter and summer precipitation (225 mm and 50 mm respectively), followed by an extremely hot summer in 2013 (where the mean July temperature was 20.1 °C). The substantially higher discharge in 2014 is attributed to extremely high snow accumulation in winter (474 mm), followed by a rainy

(71 mm) and relatively cool summer (where the mean July temperature was 14.7 °C).

Stable isotope composition in a hydrological system
Precipitation: rain and snow
From the 38 precipitation samples three have been excluded as outliers, characterized by extremely high

δ^{18}O (-10 to -5.3‰) and extremely low *D*-excess (-5 to -12‰) values, caused most likely by heavy post-precipitation evaporation effects or contamination of the samples. From the remaining 35 samples a LMWL of $\delta D = 7.06\ \delta^{18}O - 5.67$ ($R^2 = 0.99$) was calculated (table 3, figure 5). Slope and intercept differ from the Global Meteoric Water Line ($\delta D = 8.0\ \delta^{18}O + 10$), indicating the influence of secondary fractionation processes such as evaporation. Temporally irregular sampling intervals as well as seasonal factors (i.e. potential overrepresentation of summer season) might also be responsible.

The δ^{18}O of precipitation follows in general the temperature (figure 6) with a maximum value of -11.8‰ in summer 2014 and a minimum value of -28.7‰ in early winter 2013/14. For *D*-excess, the analyzed samples show distinctly higher values between 12 and 21‰ in the extended winter season (October to May) than in the summer (-4 to 14‰) where amplifying evaporation effects cannot be ruled out.

Snow cover from the watersheds
Snow cover samples collected at the gauging stations from January to April 2013 show substantial spatial and temporal variability of δ^{18}O. A general West to East trend along the 10 km transect is evident from the watershed-specific samples: the average δ^{18}O for the Westernmost Little Graviyka watershed is -27.8‰, followed by Graviyka watershed (-27.2‰), and the Easternmost Fox Creek watershed (-26.0‰). Values of δD are also declining in Easterly direction from -212‰ in Little Graviyka to 200‰ in Fox Creek watersheds (table 3). *D*-excess in most cases is close to 10‰. Values of δ^{18}O are increasing from January to April from -28 to -25‰, while *D*-excess is decreasing from 13 to 7‰ over the same period. The substantial differences in isotopic composition between rain and snow make it possible to differentiate these two sources of river flow.

Ground ice
Although the number of ground ice samples collected from the soil profile were limited, they provide general regional information on the isotopic composition of the ground ice from different depths. Stratigraphic similarity between cores of various lengths (1.2 m and 3 m) and the permafrost tunnel observations at 3–10 m depths allowed for the use of ground ice samples from multiple sources to reconstruct an isotopic profile up to 10 m depth.

Ground ice samples collected from the tundra cores indicate that the active layer is characterized by slightly heavier isotopes compared to the upper permafrost. The δ^{18}O values are decreasing slightly from -15‰ within the active layer to around -17‰ in the upper permafrost. Heavier isotope composition of the active-layer may be attributed to late-summer precipitation (-15.5 to -17‰ δ^{18}O for the second half of

September) stored within the active layer prior to freezing. *D*-excess below 8‰ within the active layer is indicative of evaporation processes likely within the active layer. Below 1–1.5 m *D*-excess is above 8‰. Samples collected from the layer of seasonal freezing in forested landscapes show almost no difference in isotopic composition compared to the tundra active layer indicating the freezing of late summer precipitation.

The deep Pleistocene permafrost is represented by nine samples collected in the permafrost tunnel at 4.5–10 m depth. It showed δ^{18}O values between -16.1 and -16.9‰ regardless of depth corresponding with *D*-excess from 10.6 to 11.9‰ (table 3). The low variability of the ground ice isotope composition may indicate a fast epigenetic freezing of limnic sediments with corresponding lowering of the groundwater table, supporting previous study of the isotope composition. Similar values of δ^{18}O in late summer precipitation and in permafrost texture ice make the separation of these two sources of water flow difficult and might present the major limitation to this study.

Ground water
Ground water collected throughout the summer season is characterized by a depleted isotopic composition relative to summer precipitation and ground ice (table 3, figure 6). From late June to late September, δ^{18}O is increasing from -19.7 to -18.9‰ corresponding with decreases in *D*-excess from 12.4 to 8.8‰ suggesting that the water originated in an aquifer likely filled with snowmelt water with increasing contributions from liquid precipitation throughout the summer. Higher δ^{18}O values in the texture ice compared to the ground water suggest no contribution of melting ice over the observational period.

Thermokarst lakes and bogs
Isotopic composition of water collected from thermokarst lakes is characterized by an isotopic composition similar to late summer precipitation with δ^{18}O from -17.7 to -16.4‰ and *D*-excess from 10.2 to 21.4‰. While δ^{18}O of the texture ice in the active layer and upper permafrost is similar to the water composition in the thermokarst bogs the mean *D*-excess of 13.8‰ and slope of 7.2‰ further suggests that late summer precipitation, and not ground ice, is the dominant water source.

Local streams
Rivers in the study area vary from less than 1 km to more than 50 km in length with corresponding watershed areas from 1 to 323 km² (table 4). The largest stream (Graviyka) is characterized by a heavier isotopic composition reflecting longer storage of water in surface (thermokarst lakes, bogs) and subsurface (ground water) reservoirs within the watershed. The isotopic composition of water in smaller streams (Fox

Table 3. Stable isotope (δ^{18}O, δD, and D-excess) minimum, mean and maximum values, standard deviations as well as slope and intercept in a δ^{18}O–δD co-isotopic plot for all sampled precipitation, watershed snow cover, water flow and river ice of the three studies rivers, thermokarst lakes and ground ice within the study area.

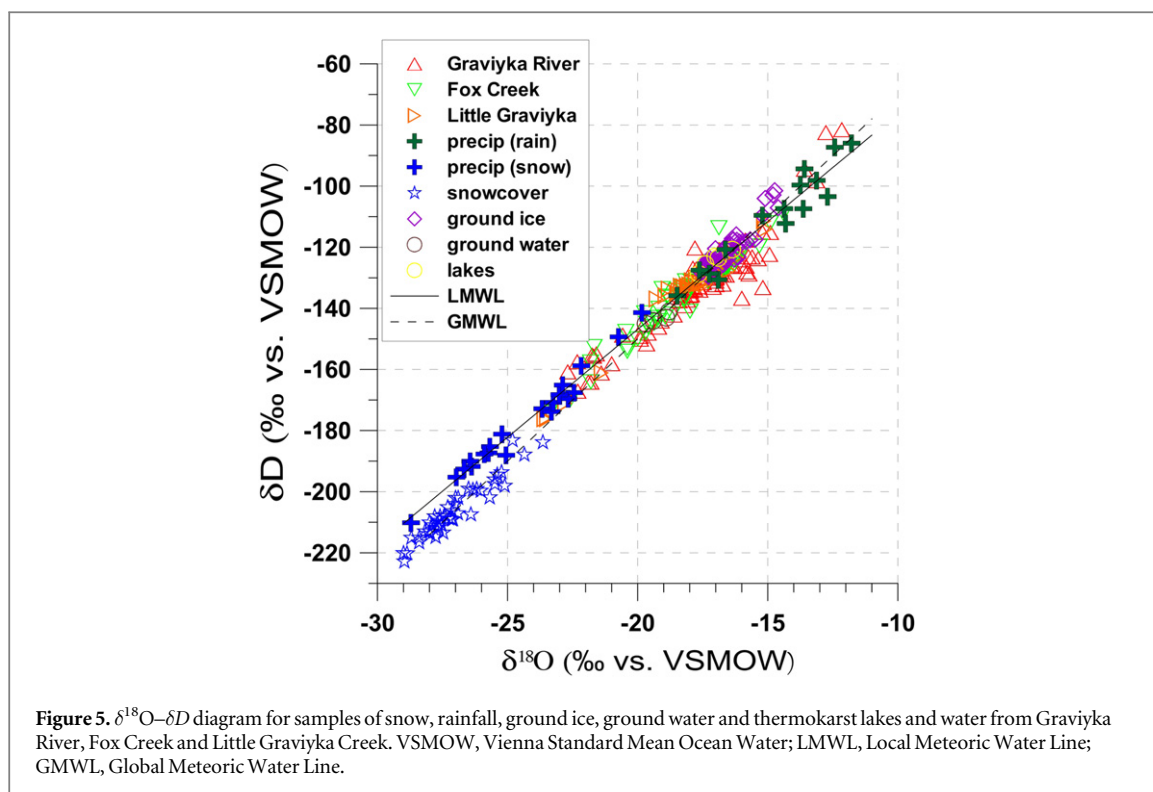| Source	N	δ^{18}O (‰)				δD (‰)				D-excess				Slope	Intercept	R^2
		Min	Mean	Max	Stdev	Min	Mean	Max	Stdev	Min	Mean	Max	Stdev			
Precipitation gauge	35	−28.7	−20.2	−11.8	5.3	−210.1	−148.4	−85.9	37.5	−1.8	13.5	21.4	6.0	7.1	−5.0	0.99
Graviyka River flow	79	−22.7	−17.6	−12.2	2.2	−167.0	−132.9	−81.4	15.9	−11.6	8.3	22.2	2.2	6.7	−14.1	0.89
Fox Creek flow	56	−23.4	−18.2	−14.4	1.9	−174.0	−135.2	−109.0	13.6	3.0	10.2	21.4	1.9	6.8	−11.5	0.94
Little Graviyaka flow	36	−23.6	−18.1	−15.1	2.0	−176.0	−133.9	−111.3	14.6	4.5	11.0	17.4	2.0	7.3	−1.1	0.97
Graviyka River snow	9	−29.0	−27.2	−24.8	1.5	−222.8	−206.2	−183.1	12.7	8.2	11.4	15.3	2.3	8.5	25.4	0.97
Fox Creek snow	8	−28.0	−26.0	−23.6	1.6	−210.3	−199.8	−183.8	10.1	3.7	8.4	14.0	3.2	6.3	−34.6	0.97
Little Graviyaka snow	9	−28.9	−27.8	−25.1	1.1	−220.1	−212.3	−198.1	6.1	2.8	9.8	14.6	3.3	5.4	−63.3	0.93
Graviyka River ice	3	−20.4	−17.1	−14.1	3.1	−157.4	−132.5	−110.0	23.8	2.8	4.4	5.5	1.4	NA	NA	NA
Fox Creek ice	2	−21.8	−17.5	−13.2	6.1	−162.0	−131.0	−100.0	43.8	5.6	9.0	12.4	4.8	NA	NA	NA
Little Graviyaka ice	6	−21.7	−17.7	−15.2	2.5	−163.0	−132.3	−113.0	18.9	8.2	9.3	10.8	1.2	7.6	2.3	1.00
Thermokarst Lake	5	−17.7	−17.0	−16.4	0.5	−128.6	−121.9	−113.6	5.5	10.3	13.8	21.4	4.4	7.2	−0.4	0.37
Spring−grownd water	4	−19.7	−19.2	−18.8	0.4	−145.0	−143.3	−141.0	1.7	8.2	10.4	12.6	1.9	3.7	−72.1	0.85
Taiga ground ice (0−0.4)	7	−16.4	−15.9	−15.0	0.6	−123.3	−119.1	−116.5	2.3	2.9	7.9	11.9	3.4	2.8	−75.3	0.46
Tundra ground ice (0−3.5 m)	40	−17.5	−16.6	−14.6	0.8	−129.5	−121.3	−101.4	6.8	6.0	11.5	16.8	2.6	8.0	11.8	0.85
Permafrost ground ice (4−10)	9	−17.1	−16.3	−15.2	0.7	−125.2	−119.1	−119.1	5.1	7.9	11.6	15.7	2.6	6.7	−9.5	0.77

Figure 5. $\delta^{18}O$–δD diagram for samples of snow, rainfall, ground ice, ground water and thermokarst lakes and water from Graviyka River, Fox Creek and Little Graviyka Creek. VSMOW, Vienna Standard Mean Ocean Water; LMWL, Local Meteoric Water Line; GMWL, Global Meteoric Water Line.

Creek and Little Gravyika) corresponds well to precipitation indicating quicker watershed drainage after each precipitation event compared to the larger Gravyika stream (figure 6). Figure 6 shows daily weather characteristics such as air temperature, precipitation, and snow accumulation, hydrochemical characteristics of waterflow in Graviyka stream (pH and EC), and the isotopic composition of precipitation and stream water from three watersheds.

It should be noted, that the regression of the isotopic composition of water from the Graviyka stream, $\delta D = 6.7\,\delta^{18}O - 14$, is similar to that of water from the Yenisei as measured 225 km downstream from the study area ($\delta D = 7.04\,\delta^{18}O - 9.32$, flux weighted $\delta^{18}O$ is -18.4‰ and δD is -139.4‰; (Yi *et al* 2012)). Figure 7 provides summary frequency distributions of $\delta^{18}O$ in water flow of the three streams with all other end-members shown on the single graph. The isotopic composition of stream water varies depending on major annual hydrological events such as spring flood, summer-fall low flow, and winter baseflow. There is a clear distinction between rain and snow; however other sources of water in a river flow have similar isotopic composition making further separation quite difficult. Despite of this limitation, the isotope data provide valuable insight into the understanding of the hydrological processes on permafrost.

Spring flood

Streams within the study area are characterized by steep maxima in discharge during the spring flood, which occurs in late May through the beginning of June. Spring floods are dominated by snowmelt water

with substantially lighter isotopic composition and higher values of D-excess (figure 6). The magnitude of the spring flood depends on the watershed characteristics (area, topography, exposure), amount of snow, rate of air temperature change, and rain intensity during the snowmelt. The onset of the flood in smaller streams precedes that of larger streams by about a week. The winter of 2014 had considerably higher snow accumulation compared to 2013 (111 and 78 cm, respectively). However, the spring flood of 2014 had a smaller magnitude as the duration of snowmelt was twice as long (20 days in 2013 and 9 in 2014). The maximum daily discharge of Graviyka River estimated for 2013 was 94 m^3 s^{-1}, while 160 m^3 s^{-1} in 2014.

The isotope composition of river flow is almost identical to the isotopic composition of the snowpack in corresponding watersheds prior to snowmelt with $\delta^{18}O$ around -24‰ to -25‰ (table 3). Isotopically depleted melting snow is mixing with enriched liquid precipitation throughout the snowmelt season resulting in a gradual increase of $\delta^{18}O$ in the waterflow. Gradual increases in temperature during the spring of 2013 and a short, but intense snowmelt is clearly seen in the isotopic curves of all three studied rivers (figure 6). However, the long spring flood of 2014, with temperatures above and below 0 °C and several rain-on-snow events, with particularly strong rain (8 mm d^{-1}) on 3 June 2014 resulted in the temporary enrichment of snowmelt water by heavy rain precipitation dividing the $\delta^{18}O$ minimum into two minima: one prior to the rain event that was produced predominantly by snowmelt, and another smaller
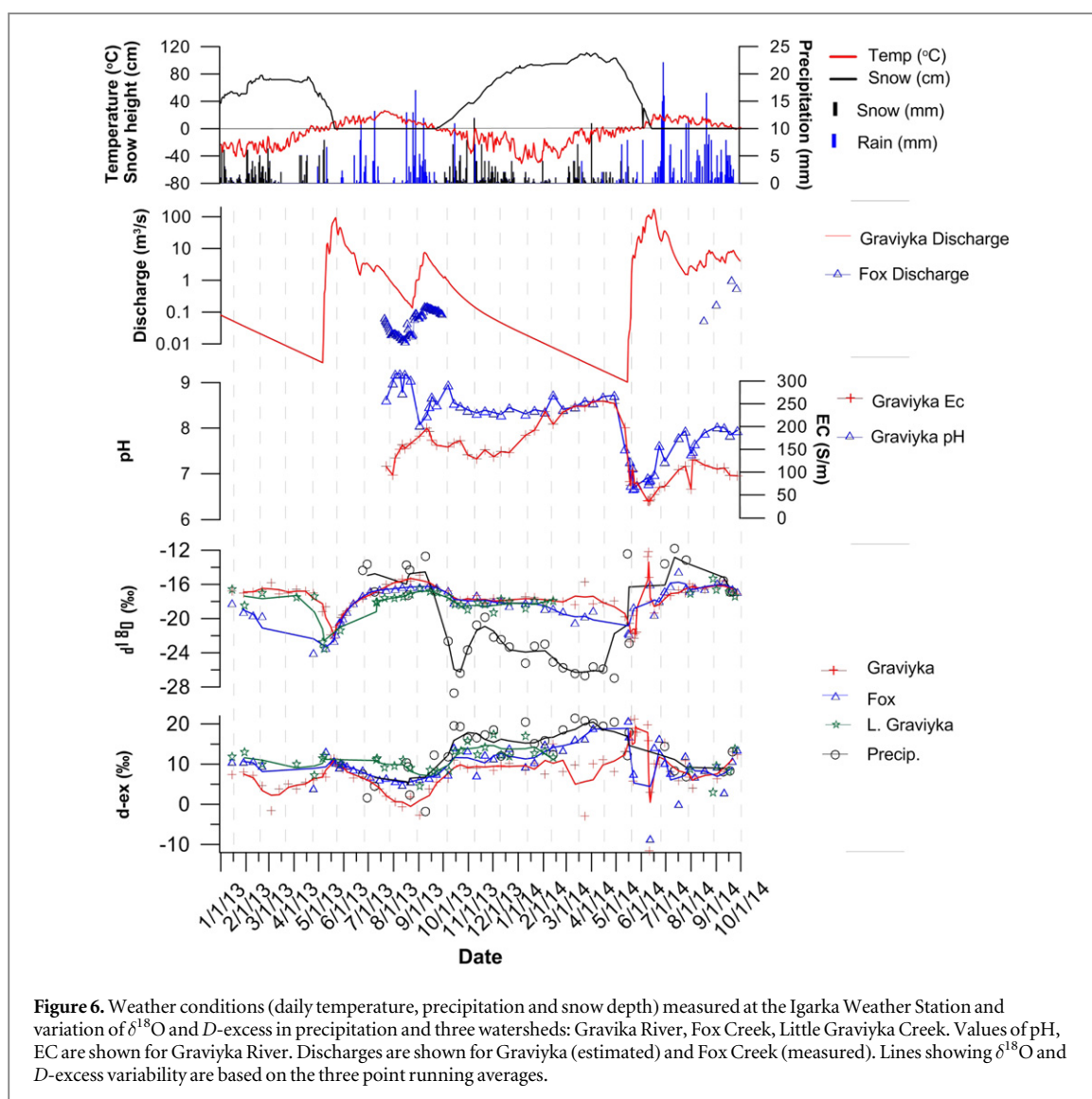
Figure 6. Weather conditions (daily temperature, precipitation and snow depth) measured at the Igarka Weather Station and variation of δ^{18}O and D-excess in precipitation and three watersheds: Gravika River, Fox Creek, Little Graviyka Creek. Values of pH, EC are shown for Graviyka River. Discharges are shown for Graviyka (estimated) and Fox Creek (measured). Lines showing δ^{18}O and D-excess variability are based on the three point running averages.

Table 4. Hydrological characteristics of the rivers in the study area and landcover classification of their watersheds.

Watershed	Length (km)	Watershed area (km^2)	Discharge[a] (m^3 s^{-1})	Tundra (%)	Taiga (%)	Soil (%)	Water (%)
Graviyka River	50.2	322.9	4.94	27	64	1	8
Fox Creek	10.5	24.29	0.388	27	69	1	2
L Graviyka Creek	0.93	1.25	0.030	7	93	0	0

[a] Graviyka discharge is estimated from the historic daily data for the 1973–1990; discharge of Fox Creek and Little Graviyka Creek is estimated based on four measurements taken in August–September 2014.

minimum later that was produced by the combination of liquid precipitation and snowmelt from snow held in watershed depressions (e.g. gullies, thermokarst). Significant decreases in EC from 250 to 40 μS and pH change from 8.7 to 7 in Graviyka River flow confirms dominating snowmelt water's contribution to river discharge. The presence of near-surface permafrost does not seem to play an important role during the snowmelt period as both permafrost and seasonal frost create an impermeable layer close to the surface allowing effective watershed drainage for all landscapes regardless of the permafrost depth.

Summer-fall flow

The frozen ground starts to thaw by the last week of May, first week of June. In forested areas with no near-surface permafrost, the layer of seasonal freezing thaws completely by the third week of July allowing the current year's precipitation to recharge water previously stored in the soil. The downward movement of water in tundra landscapes is limited to a shallow depth by the presence of the permafrost table. However, lateral water migration is possible on slopes, especially in organic-rich soils characterized by high hydraulic conductivity. The thaw depth in areas with near-surface permafrost increases throughout the

Figure 7. Boxplots of δ^{18}O in a hydrological system: (a) rainfall, (b) snow, (c) ground ice, (d) thermokarst lakes, (e) ground water, (f) Graviyka River spring flood, (g) Graviyka River summer-fall flow, (h) Graviyka River base flow, (i) Fox Creek spring flood, (j) Fox Creek summer-fall flow, (k) Fox Creek base flow, (l) Little Graviyka spring flood, (m) Little Graviyka summer-fall flow, (n) Little Graviyka base flow.

warm season and reaches its annual maximum in the beginning of October. The active-layer thickness depends on edaphic properties of the landscape and ranges from 0.4–0.7 m in organic-rich soils, 0.8–0.9 m in loamy soils, and up to 1.0–1.5 m in proximity to large thermokarst lakes. The propagation of thawing throughout the summer season increases soil storage capacity resulting in a longer time-lag between precipitation events and increased stream discharge.

Heavier isotopic composition and lower deuterium excess of the summer streamflow suggests that liquid precipitation is the dominant source for the flow after the spring flood(s) (figures 6 and 7). Variations of EC and pH of the river flow follow the magnitude of precipitation events. On average, the discharge of Graviyka is 4.6 m^3 s^{-1}, while Fox Creek discharge is only 0.46 m^3 s^{-1}. The discharge of smaller streams responded to the precipitation events quicker and without alteration of the isotopic composition. The waterflow of the larger Graviyka River shows heavier isotope composition relative to precipitation events. This indicates that initially water is stored and subject to evaporation in numerous bogs and thermokarst lakes within the watershed prior to entering the stream. The effect of evaporation, visible in higher δ^{18}O and lower D-excess values, was most pronounced during the abnormally warm and dry summer of 2013. By contrast, it was less evident during the cooler summer of 2014.

Baseflow condition

Air temperature drops below 0 °C during the first week of October initiating seasonal freezing. Initial development of a downward migrating freezing front reflects in water flow as a general decrease of δ^{18}O by 1–1.5‰ and of δD by about 10‰, after which δ^{18}O and δD vary little during the entire winter low with

exception of late March (figure 6). The depletion of water flow isotope composition occurs due to preferential freezing of heavy isotopes during ice segregation (Konishchev *et al* 2014) and the fractionation of water due to congelation of ice formation (Vasilchuk 2011). Within the study area the isotope composition of river is complicated further by soil/groundwater intrusion on the surface of the ice and the formation of naleds (a. k.a. river icings).

Field observations during late winter—early spring show numerous events of ejection of organic-rich distinctively brown soil water flowing on the surfaces of the frozen streams. The downward propagating freezing front precludes surface water infiltration and builds up the hydrostatic pressure within the soil column. Soil water moves to the locations with smaller hydraulic head, such as streams channels, contributing to the late fall—winter increase in stream discharge. High hydraulic pressure of the stream flow under the ice was evident during several ice drilling tests conducted throughout the winter. The water was quickly ejected from the relatively small hole forming a 0.05–0.06 m thick water layer on the surface of the ice. Smaller streams of less than 1.5 m depth freeze up completely by the end of February—early March limiting water movement to taliks below the stream channel. The water commonly reaches the surface of river ice via multiple cracks. The cracks are usually found near the river banks, where excessive windblown snow cover prohibits the formation of a thick layer of river ice. By the end of the winter the ground water source is usually depleted, causing creeks to dry. The only river that is not freezing to the bottom is Graviyka. The minimum estimated discharge of 0.1–0.2 m^3 s^{-1} is found in late April and May, just before the spring flood.

Maximums of $\delta^{18}O$ observed in March of 2013 and 2014 in the Graviyka River and negative D-excess are similar to the ones observed during mid-summer suggesting that enriched summer water is stored in the watershed soil and had finally reached the water flow (figure 6). This time also corresponds to the highest level of EC of 240–260 μS and pH of 8.5–8.7. The fact that these events occurred during maximum freezing suggests that the advancing freezing front and therefore closing of the hydrological system was able to deliver the water previously stored in the soil to the river flow.

Role of permafrost in hydrology in changing climatic conditions

Observational results suggest that permafrost plays an important role in the maintenance of discharge during the cold months (Walvoord and Striegl 2007, Walvoord *et al* 2012, Woo 2012, Jorgenson *et al* 2013, Quinton and Baltzer 2013). The short observational record prevents long-term analysis of the hydrologic and permafrost systems' behavior within the study area. However, indirect evidence, described above, can be used to infer the effects of long-term climate and permafrost changes on the hydrologic regime in the Igarka region.

The changes in groundwater storage resulting from thickening of the permafrost active layer in tundra landscapes and the thinning of the seasonal freezing layer in forested landscapes can, at least partially, explain the changes to the hydrologic regime evident on figure 3. Progressive lowering of the permafrost table and decreases in depth of seasonal freezing during the 1980s promoted more water storage in deeper soil layers during late summer months (July and August) and increasingly delayed release of water into the streams relative to the colder 1970s. The development of residual thaw layer above the permafrost in late 1980s allowed for soil water migration during the winter months, contributing to increases in winter flow. Our field observations of ground water ejections during the winters of 2013 and 2014, a heavy isotopic composition and high EC of winter flow in the Graviyka during the period of maximum freezing, formation of extensive river icings (naleds) in smaller streams further confirm redistribution of summer precipitation toward discharge during winter months.

Enhanced release of relatively warm soil water into streams during winter months can potentially contribute to decreases in river ice thickness (Jones *et al* 2013) further promoting increases of winter discharge. A recent study showed that the duration of ice conditions across Russian Arctic rivers have decreased over the last fifty years (Shiklomanov and Lammers 2014). For the Yenisei River near Igarka, the river ice formation is initiated 2 days later, while the river ice melts 5 days earlier and the maximum ice thickness decreased from about 1.3 m to 0.8 m.

Although this study did not find any direct evidence of ground ice melt in streams within the study area it is likely that melting ground ice can contribute to river discharges under continuing climate change, especially in areas with the presence of ice-wedges and tabular ground ice, such as Yenisei North. Ice wedges form during snowmelt by the immediate refreezing of melt water in thermal contraction cracks. Their isotopic composition is indicative of winter temperatures (Meyer *et al* 2015) and therefore differs considerably from summer precipitation. Reflecting the different climate conditions during ice wedge formation, isotopic differences can be used to distinguish Holocene from Late Pleistocene ice wedges. The closest ice wedges studied in detail (Cape Sopochnaya Carga, 71 53' N, 82 40 E, 500 km, downstream on the Yenisei River, revealed mean $\delta^{18}O$ (δD) values of $-20.3‰$ ($-154.4‰$) for Holocene and $-26.0‰$ ($-199.5‰$) for Late Pleistocene ice wedges (Streletskaya *et al* 2011). Tabular massive ground ice of likely glacier origin on the banks of the Yenisei River (namely the 'Ice mountain' 100 km upstream) exhibit a mean $\delta^{18}O$ value of $-20.4‰$ (Vaikmae *et al* 1988). As these isotope values are significantly lower than that of summer precipitation the impact of melting massive ground ice should be better detectable in river water relative to the texture ground ice.

Conclusions

Rivers and creeks in the discontinuous permafrost region have characteristic intra-annual variability evident from changes in hydrological characteristics and the stable isotope composition of river water. Heavy isotope composition during the summer is attributed to enriched summer precipitation, commonly amplified by evaporation effects for rivers with watersheds occupied by thermokarst lakes and bogs allowing for the storage of water from precipitation. Watersheds freezing in the fall results in a slight decrease in isotopic composition of river water relative to the late summer values due to the formation of segregation ice. Isotopic composition of water during winter low flow is primarily attributed to isotopically enriched ground water from the late summer precipitation events. Lighter values in spring are attributed to snow melt.

Permafrost plays an important role in the hydrology of the study area. Increases in air temperature observed in the study area resulted in permafrost degradation and shallower seasonal freezing of the ground which is evident from soil temperature measurements, permafrost and active-layer monitoring and analysis of satellite imagery. The lowering of the permafrost table and thinning seasonal freezing layer have resulted in increased soil storage capacity and allow the redistribution of late summer precipitation

towards late winter–spring months when the freezing front is at its maximum depth.

While the study did not find a direct contribution of melting ground ice to river flow, the redistribution of summer precipitation to the winter low, observed ejections of ground water and the formation of naleds (river icings) provide evidence for the indirect influence of permafrost degradation to river discharge, supporting findings of changes of the terrestrial water budget of the Eurasian Pan-Arctic from GRACE satellite (Landerer *et al* 2010).

These results have improved our understanding of interactions between permafrost and hydrology in small arctic streams and of the relative contributions from different sources to overall river discharge. They can also be useful for improving the representation and parameterization of freeze-thaw processes in various hydrological models and as validation for isotope models in the Arctic.

Acknowledgments

Appendix

Water samples for stable isotope analysis

Water samples were collected using 0.5 liter bottles filled completely to avoid evaporation effects. Samples

Table A1. Location of the sampling sites for the stable isotope analysis.

Site name	Latitude, N	Longitude, E
Precipitation gauge	67°27′10.06″	86°32′07.09″
Graviyka River	67°30′2.54″	86°34′17.47″
Little Graviyka Creek	67°28′57.76″	86°25′32.20″
Fox Creek	67°27′10.33″	86°42′17.27″
Groundwater Well	67°30′46.27″	86°36′13.79″
Soil borehole—tundra	67°28′04.13″	86°30′20.55″
Soil borehole—forest	67°27′54.50″	86°30′32.33″
Permafrost museum	67°27′55.31″	86°36′34.75″
Thermokarst Lakes	67°28′56″	86°26′08″

of stream water were collected at 1 to 10 day intervals, depending on the rate of change in hydrologic conditions and sites' accessibility. Water sampling at other sources was conducted sporadically. Samples with high concentrations of suspended sediment were filtered. The location of sampling sites is provided in table A1.

Precipitation samples (rain and snow) were collected to determine stable isotope signatures of the atmospheric input to the hydrological system. Water samples were collected with a rain-gauge at two-week intervals over the 2013 and 2014 summers. In 2013, the rain gauge was installed in proximity to the Graviyka stream gauging station. However, due to vandalism, it was moved to the roof of the Igarka Geocryology Laboratory in 2014.

Additional snow samples were collected from all three watersheds near the corresponding gauging stations during the winter 2013/14. Snow samples were taken using a VS-43 snow-sampler and packed into sealed plastic bags. Individual samples were integrated to provide a representation of the watershed snow cover for each sampling date. Prior to analysis snow samples were melted at room temperature and the water was collected into 30 ml plastic bottles, filled completely and sealed to avoid evaporation.

Five water samples were collected from five randomly selected thermokarst lakes and bogs characteristic of the area with sizes from 5 to 15 m^2 to determine the influence of summer evaporation and potential ground ice contribution to the isotope composition of the water. All thermokarst lakes were located in Little Graviyka watershed and sampled on 24 September 2014.

Ground water samples were collected four times during summers of 2013 and 2014 from a spring located in the Graviyka watershed 6.5 km North of the town of Igarka. The spring has permanent flow during the entire year suggesting a ground water supply source similar to the Graviyka River, but problems with accessibility did not allow for sample collection from this source after the first snowfall.

Samples of river ice were collected near each of the three gauging stations twice during the winter of 2013/2014 to determine the fractionation as a result of

water freezing and to assess the groundwater contribution to ice formation in the studied streams.

To determine the stable isotope composition of the upper permafrost and seasonally frozen layer, six 1.2 m long cores were extracted from boreholes drilled in February of 2013. Three cores represented near-surface permafrost in tundra landscape and three represented the seasonally frozen layer within the birch-larch forest (figure 1). At each tundra site, ice samples were collected every 0.40 ± 0.1 m along the entire core. At forested sites seven samples were collected from the seasonally frozen layer up to 0.3–0.4 m depth. Additional permafrost samples were obtained from each stratigraphic layer of a single three-meter core extracted from the tundra in July 2013. Samples from the permafrost were collected in the permafrost tunnel under the Igarka Permafrost Museum at depths of 4.5, 7.5 and 10 m (three samples at each depth).

References

AMAP 2011 *Snow, Water, Ice and Permafrost in the Arctic* (SWIPA) (Oslo: Arctic Monitoring and Assessment Programme (AMAP))

Astakhov V and Isaeva L 1988 The 'Ice Hill': an example of 'retarded deglaciation' in Siberia *Quat. Sci. Rev.* **7** 29–40

Astakhov V and Mangerud J 2007 The geochronometric age of Late Pleistocene terraces on the lower Yenisei *Doklady Earth Sciences* (Berlin: Springer) pp 1022–6

Bassinot F C *et al* 1994 The astronomical theory of climate and the age of the Brunhes–Matuyama magnetic reversal *Earth Planet. Sci. Lett.* **126** 91–108

Bhatt U S *et al* 2010 Circumpolar Arctic tundra vegetation change is linked to sea ice decline *Earth Interact.* **14** 1–20

Callaghan T V *et al* 2011 Multi-decadal changes in tundra environments and ecosystems: synthesis of the International Polar Year-Back to the Future Project (IPY-BTF) *Ambio* **40** 705–16

Fedorov A, Ivanova R, Park H, Hiyama T and Iijima Y 2014 Recent air temperature changes in the permafrost landscapes of Northeastern Eurasia Polar *Science* **8** 114–28

Flessa H *et al* 2008 Landscape controls of CH4 fluxes in a catchment of the forest tundra ecotone in northern Siberia *Global Change Biol.* **14** 2040–56

Huitu E, Arvola L and Sonninen E 2013 Seasonal variations in stable isotope ratios of oxygen and hydrogen in two tundra rivers in NE European Russia, Isotopes in hydrology, marine ecosystems and climate change studies, *Proc. Int. Symp.* vol I pp 199–201

Jacques J M St and Sauchyn D J 2009 Increasing winter baseflow and mean annual streamflow from possible permafrost thawing in the Northwest Territories, Canada *Geophys. Res. Lett.* **36** L01401

Jones C E, Kielland K and Hinzman L D 2013 Modeling groundwater upwelling as a control on river ice thickness, *Proc. 19th Int. Northern Research Basins Symp. Workshop* (*Southcentral AK, 11–17 August 2013*) pp 107–15

Jorgenson M T *et al* 2013 Reorganization of vegetation, hydrology and soil carbon after permafrost degradation across heterogeneous boreal landscapes *Environ. Res. Lett.* **8** 035017

Klaus J and McDonnell J 2013 Hydrograph separation using stable isotopes: review and evaluation *J. Hydrol.* **505** 47–64

Konishchev V N, Golubev V N, Rogov V V, Sokratov S A and Tokarev I V 2014 Experimental study of the isotopic fractionation of watering in the process of ice segregation *Earth Cryoshere* **XVIII** 3–10

Kuznetsova T P, Rogov V V and Shpolyanskaya N A 1985 Late Pleistocene stage of cryogenesis of eatern part of West Siberia *Development of Cryolithozone of Eurasia in Late Cenozoic* (Moscow: Nauka) pp 52–67

Lacelle D and Vasil'chuk Y K 2013 Recent progress (2007–2012) in permafrost isotope geochemistry *Permafrost Periglacial Process.* **24** 138–45

Landerer F W, Dickey J O and Güntner A 2010 Terrestrial water budget of the Eurasian pan-Arctic from GRACE satellite measurements during 2003–2009 *J. Geophys. Res.: Atmos.* **115** D23115

Lebedeva L, Semenova O and Vinogradova T 2014 Simulation of active layer dynamics, upper kolyma, Russia, using the hydrograph hydrological model *Permafrost Periglacial Process.* **25** 270–80

McClelland J W, Déry S J, Peterson B J, Holmes R M and Wood E F 2006 A pan-arctic evaluation of changes in river discharge during the latter half of the 20th century *Geophys. Res. Lett.* **33** L06715

McClelland J W, Holmes R M, Peterson B J and Stieglitz M 2004 Increasing river discharge in the Eurasian Arctic: Consideration of dams, permafrost thaw, and fires as potential agents of change *J. Geophys. Res.: Atmos.* **109** D18102

Meyer H *et al* 2015 Long-term winter warming trend in the Siberian Arctic during the mid- to late Holocene *Nat. Geosci.* **8** 122–5

Nyland K 2015 *Climate- and Human- Induced Land Cover Change and its Effects on the Permafrost System in the Lower Yenisei River of the Russian Arctic* The George Washington University

Oberman N G and Shesler I G 2009 Observed and projected changes in permafrost conditions within the European North–East of the Russian Federation *Probl. Severa i Arctiki Rossiiskoy Federacii* **9** 96–106

Peel M C, Finlayson B L and McMahon T A 2007 Updated world map of the Köppen–Geiger climate classification *Hydrol. Earth Syst. Sci. Discuss.* **4** 439–73

Peterson B J *et al* 2002 Increasing river discharge to the Arctic Ocean *Science* **298** 2171–3

Quinton W and Baltzer J 2013 The active-layer hydrology of a peat plateau with thawing permafrost (Scotty Creek, Canada) *Hydrogeology J.* **21** 201–20

Rodionov A *et al* 2007 Organic carbon and total nitrogen variability in permafrost-affected soils in a forest tundra ecotone *Eur. J. Soil Sci.* **58** 1260–72

Romanovsky V *et al* 2010 Thermal state of permafrost in Russia *Permafrost Periglacial Process.* **21** 136–55

Schneider A 2012 Monitoring land cover change in urban and peri-urban areas using dense time stacks of Landsat satellite data and a data mining approach *Remote Sens. Environ.* **124** 689–704

Sergievskaya Y, Poznarkova S and Tananaev N 2012 Monitoring of the depth of seasonal thawing in the lower reaches of the Yenisey river at site CALM R-40 of Igarka town, *10th Int. Conf. on Permafrost: Resources and Risks of Permafrost Areas in a Changing World vol 4/1 Extended Abstracts* (Ekaterinburg, Russia: Fort Dialog-Iset) pp 514–5

Shiklomanov A and Lammers R 2014 River ice responses to a warming Arctic—recent evidence from Russian rivers *Environ. Res. Lett.* **9** 035008

Shiklomanov A I and Lammers R B 2013 Changing discharge patterns of high-latitude rivers *Climate Vulnerability* ed R Pielke (Oxford: Academic)

Shiklomanov A I *et al* 2013 Hydrological changes: historical analysis, contemporary status, and future projections , *Regional Environmental Changes in Siberia and their Global Consequences* (Berlin: Springer) pp 111–54

Shiklomanov N, Streletskiy D and Nelson F 2012 Northern Hemisphere Component of the Global Circumpolar Active Layer Monitoring (CALM) Program, *Proc. 10th Int. Conf. on Permafrost* (*Salekhard, Russia*) pp 377–82

Shur Y and Zhestkova T 2003 Cryogenic structure of a glacio-lacustrine deposit, *Proc. 8th Int. Conf. on Permafrost* (*Zurich, Switzerland*) pp 1051–6

Sjöberg Y, Frampton A and Lyon S W 2013 Using streamflow characteristics to explore permafrost thawing in Northern Swedish catchments *Hydrogeology J.* **21** 121–31

Streletskaya I, Vasiliev A and Meyer H 2011 Isotopic composition of syngenetic ice wedges and palaeoclimatic reconstruction, western Taymyr, Russian Arctic *Permafrost Periglacial Process.* **22** 101–6

Streletskiy D, Anisimov O and Vasiliev A 2014 Permafrost degradation *Snow and Ice-Related Hazards, Risks, and Disasters* ed W Haeberli and C Whiteman (Oxford: Elsevier) pp 303–44

Stroeve J C *et al* 2012 The Arctic's rapidly shrinking sea ice cover: a research synthesis *Clim. Change* **110** 1005–27

Sugimoto A and Maximov T 2012 Study on hydrological processes in Lena River Basin using Stable Isotope Ratios of River Water *Monitoring Isotopes in Rivers: Creation of the Global Network of Isotopes in Rivers* (*GNIR*) p 41

Tyrtikov A P 1964 Perennially frozen ground and vegetation *Technical Translation* National Research Council Canada p 34

Vaikmae R, Solomatin V and Karpov Y 1988 Oxygenisotopic composition of some massive ground ice layers in the north of west Siberia *Proc. 5th Int. Conf. on Permafrost* (*Trondheim, Norway*) pp 484–8

Vasil'chuk Y K 1989 *Lower Yenisey Region. West Siberia. Geocryology of the USSR* (Moscow: Nedra)

Vasilchuk Y K 2011 Experimental study of isotopic fractionation in water during congelation ice formation *Earth Cryosphere* **XV** 51–5

Walvoord M A and Striegl R G 2007 Increased groundwater to stream discharge from permafrost thawing in the Yukon River basin: potential impacts on lateral export of carbon and nitrogen *Geophys. Res. Lett.* **34** L12402

Walvoord M A, Voss C I and Wellman T P 2012 Influence of permafrost distribution on groundwater flow in the context of climate-driven permafrost thaw: example from Yukon Flats Basin, Alaska, United States *Water Resour. Res.* **48** W07524

Welp L *et al* 2005 A high-resolution time series of oxygen isotopes from the Kolyma River: implications for the seasonal dynamics of discharge and basin-scale water use *Geophys. Res. Lett.* **32** L14401

Woo M-K 2012 *Permafrost Hydrology* (Berlin: Springer) p 563

Yi Y *et al* 2012 Isotopic signals (18O, 2H, 3H) of six major rivers draining the pan-Arctic watershed *Glob. Biogeochemical Cycles* **26** GB1027

Yi Y, Gibson J J, Hélie J-F and Dick T A 2010 Synoptic and time-series stable isotope surveys of the Mackenzie River from Great Slave Lake to the Arctic Ocean, 2003 to 2006 *J. Hydrol.* **383** 223–32

Zepalov F N, Grebenets V I, Streletskiy D A and Shiklomanov N I 2008 Active-layer monitoring at a new CALM Site, Taimyr Peninsula, Russia, *Proc. 9th Int. Conf. on Permafrost* (*Fairbanks, Alaska, 29 June– 3 July 2008*) vol 2 pp 2037–42